Fluorescence Quenching by Pyridine and Derivatives Induced by Intermolecular Hydrogen Bonding to Pyrrole-Containing Heteroaromatics†

Jerzy Herbich,*,‡ Michał Kijak,‡ Anna Zielińska‡ Randolph P. Thummel,§ and Jacek Waluk*,‡

Institute of Physical Chemistry, Polish Academy of Sciences, Kasprzaka 44, 01-224 Warsaw, Poland, and Department of Chemistry, University of Houston, Houston, Texas 77204-5003

Received: July 3, 2001; In Final Form: October 31, 2001

Photophysical studies of a series of over 20 compounds based on pyrrole, indole, and carbazole chromophores were carried out in protic, nonpolar, and polar solvents. Absorption spectra revealed the formation of ground-state hydrogen bonding with protic solvent partners. The equilibrium constants were determined by spectrophotometric titration. Strong fluorescence quenching was observed when azaaromatic proton acceptors, pyridine and quinoline, were used as protic solvents. No quenching occurs for nonaromatic protic partners such as dimethyl sulfoxide, morpholine, and piperidine, even though the ground-state equilibrium constants are not smaller. The rates of quenching in pyridine solutions at 293 K span a range from 1.2×10^9 to 5.9×10^{10} s^{-1} and are sensitive to minor structural variations. The mechanism of quenching involves an electron transfer from a photoexcited chromophore to a hydrogen-bonded partner, followed by a rapid internal conversion (back electron transfer) to the ground state. The quenching rates are larger for systems with stronger hydrogen bonds. This model was confirmed by theoretical time-dependent DFT and semiempirical studies, in which the pattern of excited states of an isolated chromophore was compared with that of a hydrogen-bonded pyridine complex. For the latter, low-lying charge transfer (CT) states were predicted, with an electron transferred to pyridine.

1. Introduction

The process of fluorescence quenching, occurring as a result of intermolecular hydrogen bonding, is a well-known phenomenon.[1−4] Numerous studies by Mataga and co-workers[5−13] have been devoted to the case when both the proton donor (D) and acceptor (A) atoms belong to π-electronic systems. A scheme based on electron transfer has been proposed to explain the quenching process.[8−13] According to this mechanism, hydrogen bonding (HB) may lower the ionization potential of the donor and increase the electron affinity of the acceptor, thus facilitating the photoinduced electron transfer (ET) between the two moieties. This phenomenon has been observed even in systems where the standard thermodynamic estimates that assume weak D−A interactions predict large positive ΔG values for the process.[10,11]

The transition from the locally excited (LE) to the ET state need not be followed by proton transfer. For instance, in the case of 1-aminopyrene, hydrogen-bonded to pyridine, the equilibrium between D*−H···A and $D^+-H\cdots A^-$ has been observed.[11] On the other hand, in a complex between 1-pyrenol and pyridine, proton shift occurs primarily after electron transfer, which leads to a very rapid nonradiative deactivation to the ground state.[12]

We have recently investigated extensively the mechanism of excited-state double proton transfer (ESDPT) in alcohol complexes of bifunctional azaaromatic compounds, containing both pyridine and pyrrole-type nitrogen atoms.[14−23] ESDPT was observed in cases when the molecular topology was appropriate for the formation of cyclic, doubly hydrogen-bonded complexes. No proton transfer was detected when the proton donor and acceptor groups were spaced too far apart for formation of the cyclic complex. However, we observed that the properties of all the studied molecules that contained the NH group were changed in pyridine solutions.[15] In the ground state, the formation of hydrogen-bonded complexes was detected. In pyridine solutions, the excited-state characteristics showed a large decrease of fluorescence quantum yields and lifetimes.

In this work, we present the results of stationary and time-resolved photophysical studies for a series of over 20 azaaromatic compounds based on pyrrole, indole, and carbazole chromophores. Their structures are presented in Chart 1. The focus of the work is on the quantitative characterization of the photophysical parameters and on the mechanism of fluorescence quenching by pyridine and related azaaromatic proton acceptors. All the NH-containing molecules have their fluorescence quantum yield strongly reduced in the presence of pyridine and related aromatic proton acceptors, albeit to a different degree. We find that minor perturbations in a series of structurally similar compounds can have a large impact on the quenching rate. This impact is explained by a mechanism, according to which the rate-limiting step of the quenching involves an electron transfer from the lowest locally excited singlet state to a nearby charge transfer state. The electron is translocated from an excited chromophore (NH hydrogen bond donor) into the aromatic HB acceptor. The rate of this process increases with the strength of intermolecular hydrogen bond between the two aromatic partners.

The proposed model is verified by calculations for selected representatives of the series. The excited-state parameters are computed both for an isolated molecule and for its complex

† Part of the special issue "Noboru Mataga Festschrift".

* Corresponding authors. E-mail (J.W.): waluk@ichf.edu.pl.
‡ Polish Academy of Sciences.
§ University of Houston.

10.1021/jp012515y CCC: $22.00
Published on Web 01/12/2002

CHART 1: Formulas and Acronyms of the Investigated Compounds

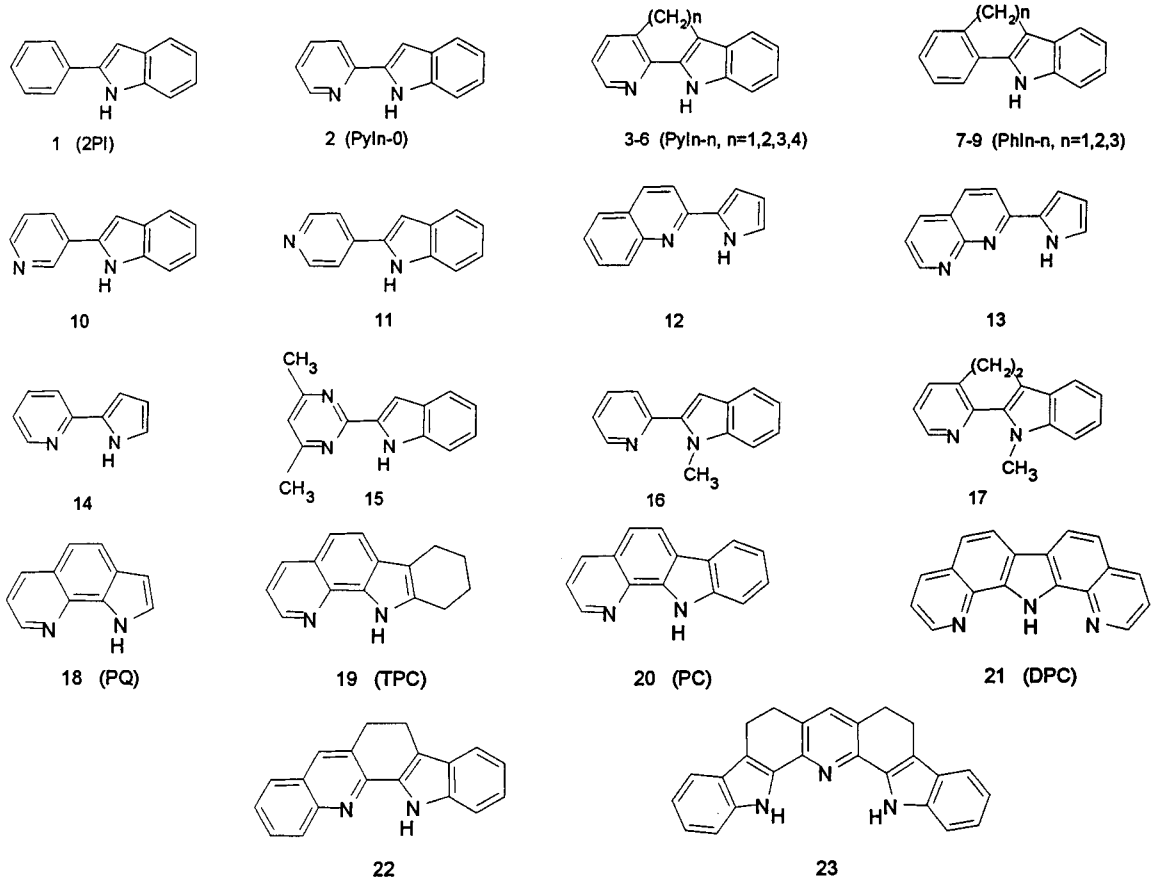

with pyridine. Low-lying CT states are found in the latter, practically isoenergetic with the lowest locally excited states.

2. Experimental Section

Syntheses and purification procedures of 2-(2′-pyridyl)indoles (**2**−**6**),[24] their 1N-methylated derivatives (**16, 17**),[16] 2-(2′-pyrrolyl)quinoline (**12**),[25] 2-(2′-pyrrolyl)-1,8-naphthyridine (**13**),[25] 2-[2′-(4′,6′-dimethylpyrimidyl)]indole (**15**),[20] 1*H*-pyrrolo[3,2-*h*]quinoline (**18,** PQ),[26] 7,8,9,10-tetrahydro-11*H*-pyrido[2,3-*a*]carbazole (**19,** TPC),[25] 11*H*-pyrido[2,3-*a*]carbazole (**20,** PC),[25] dipyrido[2,3-*a*:3′,2′-*i*]carbazole (**21,** DPC),[17] 12,13-dihydro-5*H*-indolo[3,2-*c*]acridine (**22**),[25] and 3,3′:5,3″-bis(dimethylene)-2,6-bis(2′-indolyl)pyridine (**23**)[24] were described elsewhere. The preparation of 2-(3′-pyridyl)indole (**10**),[27] 2-(4′-pyridyl)indole (**11**),[27] and 2-(2′-pyridyl)pyrrole (**14**)[28] has been reported in the literature. The preparation of 3,2′-polymethylene-2-phenylindoles (**7**−**9**) will be reported elsewhere.[29]

Solvents used for our studies, *n*-hexane, benzene, acetonitrile (ACN), dimethyl sulfoxide (DMSO), and pyridine, were of spectroscopic or fluorescence grade (Aldrich or Merck). Morpholine (POCh) and piperidine (BDH) were dried with KOH and fractionally distilled (the latter from CaH_2). Quinoline (Roth, pa) has been purified according to the procedure proposed by Calvin and Wilmarth.[30] All the solvents were checked for fluorescing impurities.

Absorption spectra were run on a Shimadzu UV 3100 and on a Shimadzu UV 2401 spectrophotometers. Steady-state fluorescence and excitation spectra were recorded on a Jasny spectrofluorimeter[31] and on an Edinburgh FS 900 CDT spectrometer. Quinine sulfate in 0.05 M H_2SO_4 ($\phi = 0.51$)[32] served as a standard for the quantum yield determinations. Fluorescence lifetimes in the nanosecond range were obtained by means of an Edinburgh FL 900 CDT time-resolved fluorometer. The spectrophotometric titration has been used to monitor the formation of hydrogen bonded complexes in mixed solvents.

Optimizations of the ground-state structures of isolated molecules and pyridine complexes were performed using a B3LYP/6-31G** model implemented in the Gaussian 98 suite of programs.[33] The Hessian matrix was checked to ensure that the calculated structure corresponds to a real minimum. These calculations were followed by TD-B3LYP/6-31G** studies of the excited-state energies. The electronic states were also calculated using semiempirical methods (INDO/S,[34] AM1,[35] PM3[36]). The latter gave results qualitatively similar to those obtained by time-dependent DFT with regard to the relative distances between LE and CT states in a series of structurally related molecules. However, the semiempirical methods yielded much higher values (about 1 eV) for the transition energies of CT states.

3. Results and Discussion

3.1. Ground-State Formation of HB Complexes. Absorption spectra of all the compounds containing the NH group change upon adding pyridine to a solution in a nonpolar solvent (Figure 1). Isosbestic points are observed, showing an equilibrium between two species.

No changes are detected upon adding pyridine to solutions of N-methylated derivatives. It is thus reasonable to attribute the spectral changes as being due to the formation of hydrogen-bonded complexes with pyridine. The red shift indicates that the hydrogen bonding strength increases upon excitation to S_1.

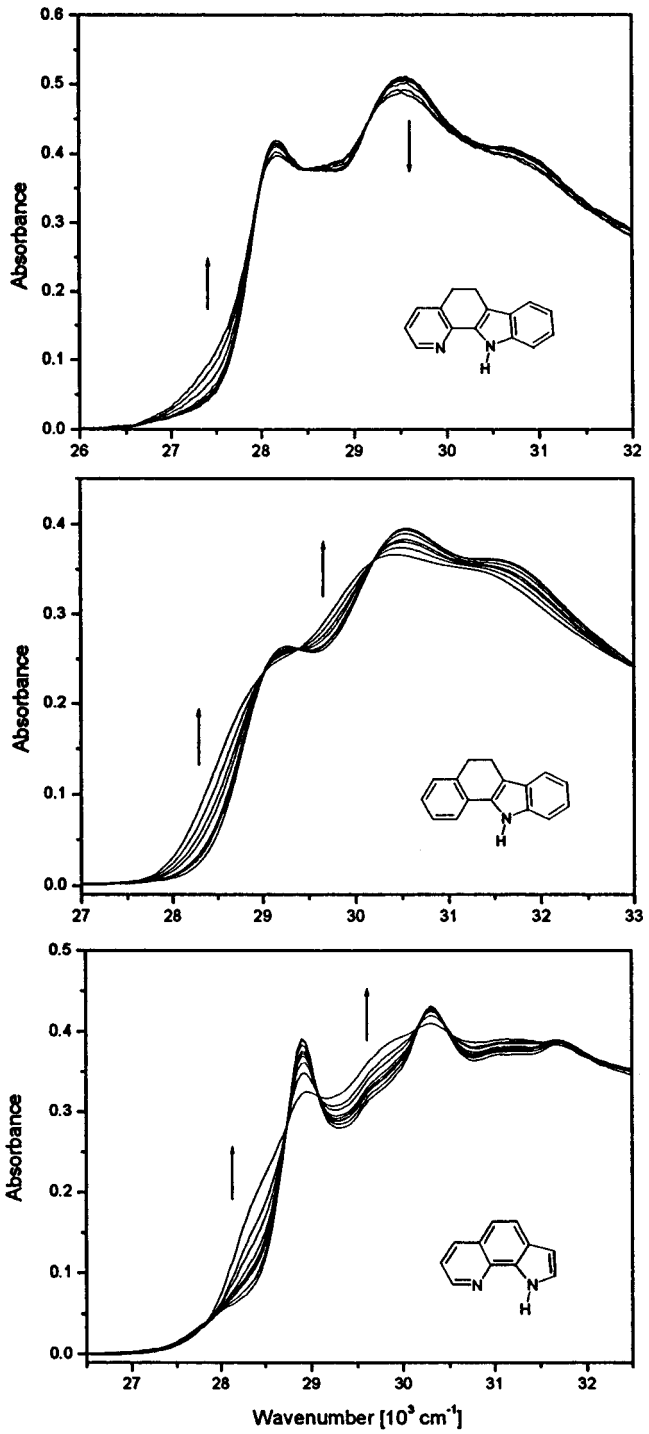

Figure 1. Spectrophotometric titration of PyIn-2 (**4**, top, $c = 2 \times 10^{-5}$ M), PhIn-2 (**8**, middle, $c = 2 \times 10^{-5}$ M), and PQ (**18**, bottom, $c = 8 \times 10^{-5}$ M) in *n*-hexane with pyridine. The arrows show spectral changes accompanying the addition of pyridine. Pyridine concentration increased up to 0.08 M for **4** and **8** and up to 0.4 M for **18**.

For a 1:1 stoichiometry, the following relation holds:[5]

$$(1 - A_0/A)/[Q] = -K_{11} + (\epsilon_{11}/\epsilon_P)K_{11}(A_0/A) \qquad (1)$$

A_o and A are the absorbances measured in the absence and presence of pyridine, respectively, [Q] is the pyridine concentration, and ϵ_{11} and ϵ_P are the extinction coefficients of the complexed and free solute molecules. Thus, the value of the ground-state equlibrium constant K_{11} may be obtained from the intercept of the plot of $(1 - A_0/A)/[Q]$ vs A_0/A (Figure 2).

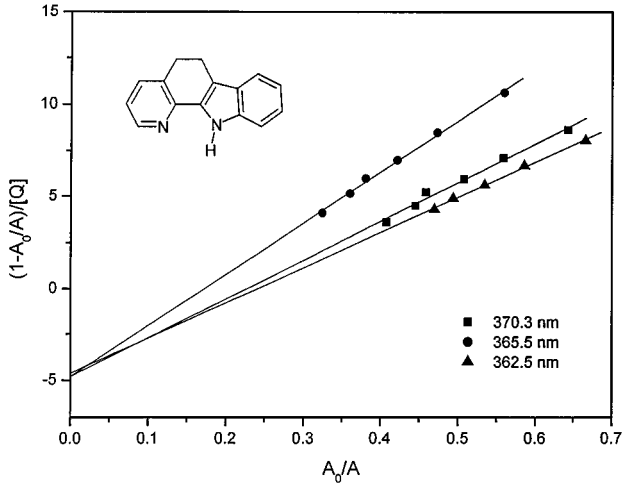

Figure 2. Determination of the equilibrium constant of the complex formation from the absorption data for PyIn-2 ($c = 2 \times 10^{-5}$ M). See text for details.

TABLE 1: Ground-State Equilibrium Constants (K_{11}, M^{-1}) at 293 K

	pyridine[a]	morpholine[a]	1-butanol[a]	DMSO[b]
PyIn-0 (**2**)	3 ± 1			
PyIn-2 (**4**)	5 ± 1	35 ± 5	40 ± 5	8 ± 1
PyIn-3 (**5**)	2 ± 1			
PyIn-4 (**6**)	3 ± 2			
PhIn-2 (**8**)	26 ± 2	31 ± 3		20 ± 2
2PI (**1**)	19 ± 3	27 ± 3		18 ± 1
PQ (**18**)	6 ± 1		180 ± 10	5 ± 1

[a] Titration in *n*-hexane solution. [b] Titration in benzene solution.

The values obtained at 293 K are shown in Table 1. For most of the compounds in this study, we have previously demonstrated the formation of ground-state HB complexes with alcohols and other proton acceptors, such as DMSO. Inspection of the equilibrium constants in Table 1 shows that the values for 2-(2′-pyridyl)indoles and pyridine are similar or smaller than those obtained for other, nonaromatic HB partners, such as DMSO and morpholine.

3.2. Quenching of Fluorescence by Pyridine and Related Compounds. Photophysical parameters, determined in nonpolar, polar aprotic solvents, and pyridine, are presented in Table 2. All the NH-containing molecules reveal the same pattern of fluorescence quantum yields and lifetimes in the presence of pyridine. As an illustration, Figure 3 shows the room-temperature fluorescence spectra of PyIn-2 (**4**), PhIn-2 (**8**), and PQ (**18**) in a nonpolar solvent, *n*-hexane, a polar aprotic solvent, acetonitrile, and two protic solvents, DMSO and pyridine. The shape and location of the fluorescence maxima in the latter two solvents are similar. However, for pyridine the quantum yield is much lower and the excited-state lifetime much shorter. No such effects are observed for DMSO. The quenching of fluorescence could be monitored by adding pyridine or a related HB acceptor to a nonpolar solution. Figure 4 shows the decrease of fluorescence intensity caused by adding pyridine and quinoline to a solution of PyIn-2 (**4**) in *n*-hexane. It is clearly seen that quinoline is a better quencher than pyridine. The pK_a values of pyridine and quinoline are very similar (5.2 and 4.9, respectively[37]), whereas their reduction potentials are not. Quinoline is a much better electron acceptor than pyridine (reduction potentials $E_{1/2}$(SCE) are −2.0 and −2.66 V, respectively[38]). Thus, this comparison (and a lack of the fluorescence quenching by DMSO, $E_{1/2}$(SCE) < −2.8 V[39]) clearly shows that the quenching mechanism involves electron-transfer interac-

TABLE 2: Quantum Yields (ϕ), Fluorescence Decay Times (τ), and the Resulting Radiative (k_r, 10^8 s^{-1}) and Fluorescence Quenching (k_q, 10^9 s^{-1}) Rate Constants[a]

	solvent								
	nonpolar[b]			polar aprotic[c]			pyridine		
	ϕ[d]	τ[e]	k_r	ϕ[d]	τ[e]	k_r	ϕ[d]	τ[f]	k_q
1	0.79			0.82	2.4	3.4	0.02	59	17
				0.76	2.1	3.6			
2	0.48	1.25	3.8	0.77	2.7	2.9	0.07	200	4.6
				0.53	1.8	2.9			
3	0.42	1.4	3.0	0.71	2.4	3.0	0.03	100	9.6
				0.48	1.8	2.7			
4	0.5	1.7	2.9	0.74	2.8	2.6	0.06	230	4.0
				0.38	1.75	2.2			
5	0.39	1.0	3.9	0.69	3.0	2.3	0.15	650	1.2
				0.45	1.5	3.0			
6	0.04	<0.3	>1.3	0.52	3.8	1.4	0.02	140	6.9
				0.14	0.6	2.3			
7	0.97	1.85	5.2	0.90	2.4	3.8	0.0064	17	59
				0.76[g]	2.2	3.5			
8	0.82	2.1	3.9	0.87	2.8	3.1	0.0077	25	40
				0.73[g]	2.6	2.8			
9	0.89	1.85	4.8	0.90	3.6	2.5	0.0072	29	35
				0.70[g]	2.3	3.0			
10	0.99	2.0	5.0	0.75	3.4	2.2	0.033	150	6.4
				0.98[g]	3.4	2.9			
11	0.83	1.6	5.2	0.82	3.0	2.7	0.038	140	6.8
				0.88[g]	3.0	2.9			
12	0.055	<0.4	>1.3	0.58	4.1	1.4	0.083	620	1.4
				0.33[g]	2.5	1.3			
13	0.019	0.5	0.4	0.75	5.8	1.3	0.034	260	3.7
				0.55[g]	4.5	1.2			
14	0.011	<0.4	>0.3	0.48	2.5	2.0	0.010	50	20
15	0.62	1.7	3.6	0.60	3.0	2.0	0.028	140	6.8
				0.70[g]	2.4	2.9			
16	0.51	1.9	2.7	0.75			0.77	2.8[e]	
				0.61[g]	2.5	2.4			
17	0.49			0.80			0.79	3.3[e]	
				0.61					
18	0.25	6.3	0.40	0.23	5.2	0.44	0.014	320	3
				0.16	4.3	0.37			
19	0.26	6.7	0.39	0.26	6.2	0.42	0.019	450	2
				0.17	5.0	0.34			
20	0.32	10.1	0.32	0.27	8.9	0.30	0.0034	110	9
				0.15	7.1	0.21			
21	0.27	14.0	0.19	0.29	5.3	0.55	0.004	72	14
				0.30	9.2	0.33			
22	0.62	2.7	2.3	0.66	3.3	2.0	0.10	520	1.7
				0.40[g]	2.1	1.9			
23	0.66			0.61	2.8	2.2	0.11	440	1.9
				0.63[g]	2.7	2.3			

[a] All the measurements were performed at 293 K. [b] *n*-Hexane. [c] First row, DMSO, and second row, butyronitrile solutions, unless indicated otherwise. [d] Accuracy: ±20−30%. [e] ns. [f] ps. [g] Acetonitrile solution.

tions. These, in turn are related to specific interactions, i.e., HB formation. This conclusion becomes evident when the properties of NH and N-methylated compounds are compared. No fluorescence quenching is observed for the latter (Table 2). This result eliminates the possibility of quenching being due to the formation of a non-hydrogen-bonded exciplex, which is an important result, since such exciplexes are known for indole and its alkylated derivatives.[40] The proposed mechanism is supported by the finding that, contrary to the strong effect in pyridine, the fluorescence quantum yields of 2PI (**1**) and PhIn-2 (**8**) do not change upon adding morpholine or piperidine to a nonpolar solution. The latter nonaromatic HB acceptors (which form ground-state hydrogen-bonded complexes, Table 1) are much stronger bases (the pK_a values are 8.3 and 11.1, respectively[37]) and much worse electron acceptors than pyridine and quinoline.

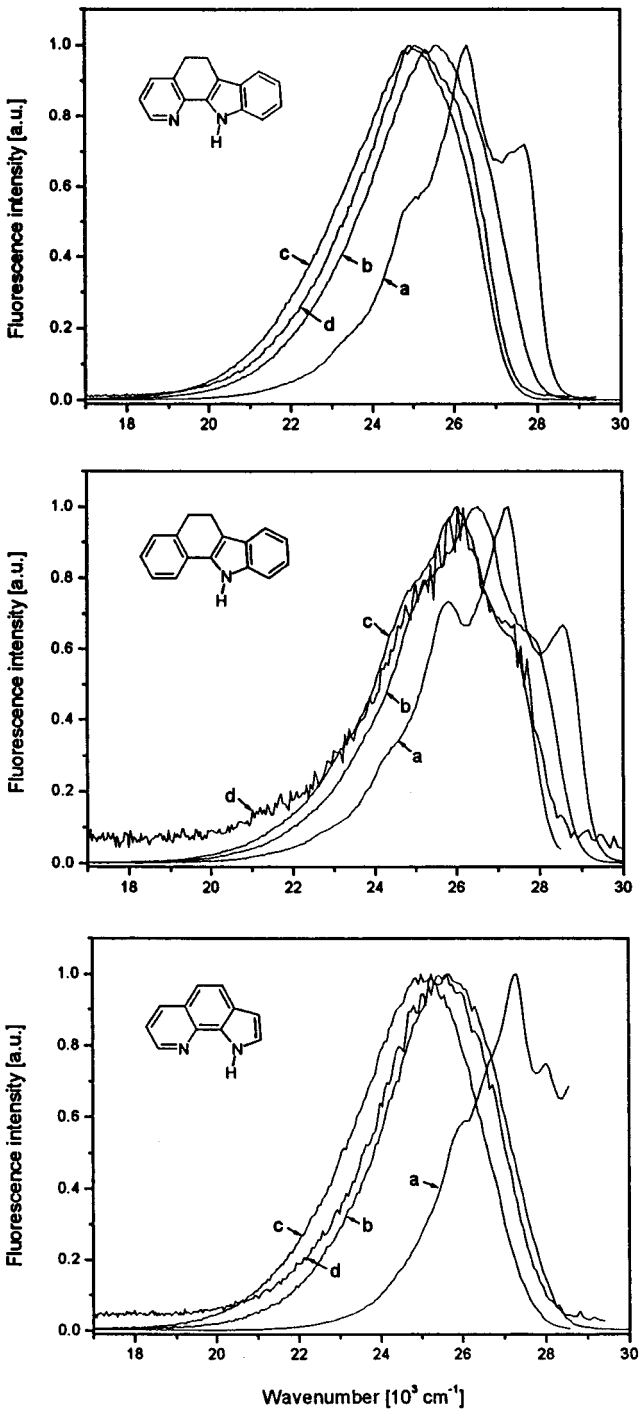

Figure 3. Fluorescence spectra of PyIn-2 (**4**, top, $c = 2 \times 10^{-5}$ M, $\lambda_{exc} = 340$ nm), PhIn-2 (**8**, middle, $c = 2 \times 10^{-5}$ M, $\lambda_{exc} = 330$ nm), and PQ (**18**, bottom, $c = 7 \times 10^{-5}$ M, $\lambda_{exc} = 330$ nm) at 293 K in *n*-hexane (a), acetonitrile (b), DMSO (c), and pyridine (d).

The quantitative analysis of the data presented in Figure 4 shows that the quenching is not purely static. Assuming that the fluorescence intensity, I, is mostly due to the uncomplexed molecules allows one to determine the equilibrium constants for complex formation from the plot of $(I_0 - I)/I$ vs the quencher concentration (I_0 is the intensity in the absence of the quencher). The values obtained for PyIn-2 (**4**), 33 M^{-1} for pyridine and 85 M^{-1} for quinoline, are much higher than 5 M^{-1}, the value for the ground-state equilibrium. Thus, the presence of the dynamic quenching is obvious.

The values of fluorescence quantum yields and fluorescence quenching rates are shown in Table 2. The latter

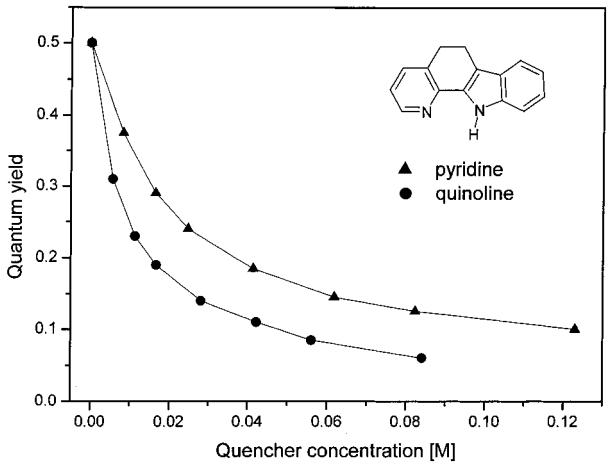

Figure 4. Changes of fluorescence quantum yield upon adding pyridine and quinoline to a 2×10^{-5} M solution of PyIn-2 (**4**) in *n*-hexane.

TABLE 3: Calculated (TD-B3LYP/6-31G) Energies (E, 10^3 cm^{-1}) and Oscillator Strengths (f) of the Lowest Excited States for an Isolated Molecule 18 and for Its 1:1 Complex with Pyridine**

	isolated molecule		complex		
	E	f	E	f	description
1	31.7	0.019	30.8	0.020	LE
			31.5	0.001	CT
2	32.7	0.030	31.8	0.035	LE
			32.2	0.004	CT
			35.1	0.001	LE (pyridine)
			35.8	0.001	CT
3	37.4	0.003			LE (nπ*)
4	38.9	0.080	37.9	0.061	LE
5	40.6	0.499	39.9	0.409	LE
6	43.0	0.000	43.9	0.000	LE (nπ*)
7	45.7	0.215	45.4	0.223	LE

were obtained using the equation

$$k_q = k_r(1/\phi - 1/\phi^0) \qquad (2)$$

where k_r is the radiative rate constant of fluorescence and ϕ and ϕ^0 are the fluorescence quantum yields measured in the presence and absence of the quencher, respectively. For the latter case, fluorescence quantum yields in DMSO were used. The k_r values were also obtained from the data for DMSO solutions, using the standard formula $k_r = \phi^0/\tau^0$; τ^0 is the measured fluorescence decay time.

The data presented in Table 2 show that the fluorescence quenching rate is quite sensitive even to minor structural details. Particularly outstanding is the comparison of the members of the series of 2-(2′-pyridyloindoles) and the related phenylindoles: the lowest quenching rate is obtained for PyIn-3 (**5**) which also reveals the smallest K_{11} value. The explanation for varying k_q rates may be found in the strength of hydrogen bond between the two partners: compared to pyridylindoles, PhIn-2 and 2PI reveal much higher values of both quenching rates and ground-state association constants.

3.3. Calculations and Analysis of Excited-State Patterns. Table 3 presents the results of TD-B3LYP/6-31G** calculations of the lowest excited singlet states performed for an isolated molecule of PQ and for its complex with pyridine. The optimized structure of the complex is presented in Figure 5. The two aromatic moieties are nearly coplanar (it should be noted that, due to steric reasons, this cannot be the case with quinoline complex).

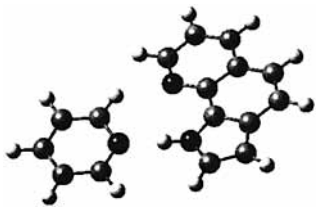

Figure 5. Optimized structure of the complex of PQ (**18**) with pyridine.

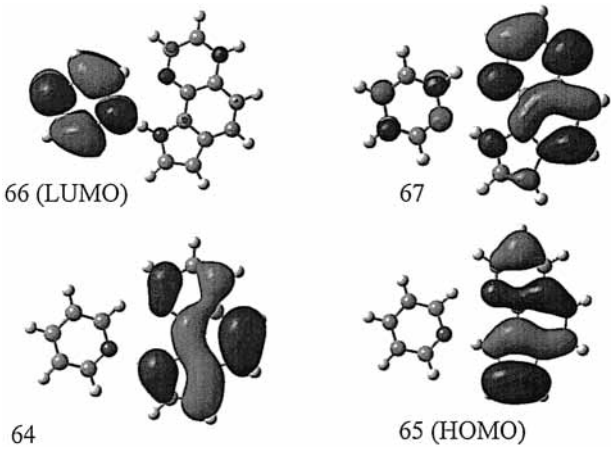

Figure 6. Orbitals involved in the lowest CT transition of a PQ:pyridine complex.

In the pyridine complex, the calculations predict the presence of several low-lying CT states. The lowest one is predicted to lie in the vicinity of the lowest locally excited state. This CT state corresponds to the transfer of an electron from an orbital localized on PQ (65, HOMO) to an orbital localized on pyridine (66, LUMO). The shapes of the two highest occupied and two lowest unoccupied orbitals in the complex with pyridine are presented in Figure 6. According to calculations, complexation of pyridine should not lead to significant changes in the transition energies of a parent chromophore. This is indeed observed. The positions of optically allowed transitions predicted by calculations agree nicely with the results obtained by absorption and magnetic circular dichroism experiments.[41]

Similar results were obtained using TD-B3LYP/6-31G** for PyIn-2 and PyIn-3. For both molecules, the lowest calculated CT state in the hydrogen-bonded complex with pyridine was predicted to lie slightly (about 1000 cm^{-1}) below the lowest locally excited state. These results confirm the notion that the mechanism of quenching involves the population of a CT state, accessible after excitation to an LE state. Interestingly, the excited state patterns calculated by semiempirical methods also predicted the presence of the CT states, albeit at much higher energies than obtained using TD DFT (about 1 eV above the locally excited states).

3.4. Mechanism of Fluorescence Quenching. All the experimental and computational results are compatible with a mechanism, according to which fluorescence quenching involves transfer of an electron from an initially excited chromophore to a pyridine (quinoline) moiety. The presence of low-lying CT states was predicted by calculations. Because of extremely small transition intensities, these states are not likely to be observed in absorption. It should be noted that due to their larger dipole moments the CT states should be stabilized in polar solvents to a much higher degree than the LE transitions.

One could consider that the "dark" CT state could be detected by transient absorption. However, our transient picosecond studies for pyridine solutions[42] have not detected the presence

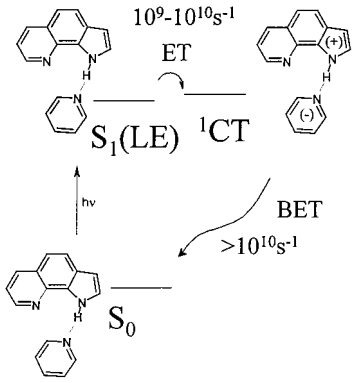

Figure 7. Mechanism of fluorescence quenching (ET, electron transfer; BET, back electron transfer).

of any transient band in the visible region that could be assigned to a CT state. Also, no spectral changes were observed that would indicate a proton transfer along the hydrogen bond. It is thus likely that the back-electron-transfer rate from a CT state is larger than the rate of the CT state formation. This puts a lower limit of about 10^{10}−10^{11} s^{-1} for the back-ET rates. Such a rapid electron-transfer process could be due to the fact that the promoting modes may be related to the hydrogen bonding between the two partners. Both anharmonicity and the large value of the NH vibration frequencies should contribute to a rapid ET process.

The proposed scheme of fluorescence quenching is presented in Figure 7. Further studies are planned to explore the mechanism of fluorescence quenching in more detail. As a first priority, the temperature dependence of the quenching kinetics will be determined. If detected in low-temperature solutions and the solid phase, the process could be investigated for cold hydrogen-bonded complexes, isolated in supersonic beams or inert matrixes.

Acknowledgment. This work was partly sponsored by Grants 3T09A 063 14 and 7 T09A 024 20 from the Polish Committee for Scientific Research and also by the National Science Foundation (Grant CHE-9714998) and the Robert A. Welch Foundation (Grant E-621) to R.P.T. We thank Dr. Andrzej Kapturkiewicz for stimulating discussions.

References and Notes

(1) Mataga, N.; Kaibe, Y.; Koizumi, M. *Nature* **1955**, *175*, 731.
(2) Rehm, D., Weller, A. *Isr. J. Chem.* **1970**, *8*, 259.
(3) Yatsuhashi, T,; Inoue, H. *J. Phys. Chem. A* **1997**, *101*, 8166.
(4) Biczók, L.; Valat, P.; Wintgens, V. *Phys. Chem. Chem. Phys.* **1999**, *1*, 4759.
(5) Mataga, N.; Tsuno, S. *Naturwissenschaften* **1956**, *10*, 305; *Bull. Chem. Soc. Jpn.* **1957**, *30*, 368; *Bull. Chem. Soc. Jpn.* **1957**, *30*, 711.
(6) Mataga, N. *Bull. Chem. Soc. Jpn.* **1958**, *31*, 481.
(7) Mataga, N.; Torihashi, Y.; Kaifu, Y. Z. *Phys. Chem. (Frankfurt/Main)* **1962**, *34*, 379. Mataga, N.; Tanaka, F.; Kato, M. *Acta Phys. Pol.* **1968**, *34*, 733.
(8) Ikeda, N.; Okada, T.; Mataga, N. *Chem. Phys. Lett.* **1980**, *69*, 251; *Bull. Chem. Soc. Jpn.* **1981**, *54*, 1025.
(9) Martin, M. M.; Ware, W. R. *J. Phys. Chem.* **1978**, *82*, 2770. Martin, M. M.; Miyasaka, H.; Karen, A.; Mataga, N. *J. Phys. Chem.* **1985**, *89*, 182.
(10) Martin, M. M.; Ikeda, N.; Okada, T.; Mataga, N. *J. Phys. Chem.* **1982**, *86*, 4148.
(11) Ikeda, N.; Miyasaka, H.; Okada, T.; Mataga, N. *J. Am. Chem. Soc.* **1983**, *105*, 5206. Miyasaka, H.; Tabata, A.; Kamada, K.; Mataga, N. *J. Am. Chem. Soc*. **1993**, *115*, 7335.
(12) Miyasaka, H.; Tabata, A.; Ojima, S.; Ikeda, N.; Mataga, N. *J. Phys. Chem.* **1993**, *97*, 8222.
(13) Mataga, N.; Miyasaka, H. *Prog. React. Kinet.* **1994**, *19*, 317 and references therein.
(14) Herbich, J.; Rettig, W.; Thummel, R. P.; Waluk, J. *Chem. Phys. Lett*. **1992**, *195*, 556.
(15) Herbich, J.; Waluk, J.; Thummel, R. P.; Hung, C.-Y. *J. Photochem. Photobiol., A* **1994**, *80*, 157.
(16) Herbich, J.; Hung, C.-Y.; Thummel, R. P.; Waluk, J. *J. Am. Chem. Soc.* **1996**, *118*, 3508.
(17) Herbich, J.; Dobkowski, J.; Thummel, R. P.; Hedge, V.; Waluk, J. *J. Phys. Chem. A* **1997**, *101*, 3508.
(18) Kyrychenko, A.; Herbich, J.; Izydorzak, M.; Gil, M.; Dobkowski, J.; Wu, F.; Thummel, R. P.; Waluk, J. *Isr. J. Chem.* **1999**, *39*, 309.
(19) Kyrychenko, A.; Herbich, J.; Izydorzak, M.; Wu, F.; Thummel, R. P.; Waluk, J. *J. Am. Chem. Soc.* **1999**, *121*, 11179.
(20) Kyrychenko, A.; Herbich, J.; Wu, F.; Thummel, R. P.; Waluk, J. *J. Am. Chem. Soc*. **2000**, *122*, 2818.
(21) Kyrychenko, A.; Stepanenko, Y.; Waluk, J. *J. Phys. Chem. A* **2000**, *104*, 9542.
(22) Waluk, J. *Conformational Aspects of Intra- and Intermolecular Excited-State Proton Transfer* in *Conformational Analysis of Molecules in Excited States*; Waluk, J., Ed.; Wiley-VCH: Weinheim, Germany, 2000; pp 57−111.
(23) Marks, D.; Zhang, H.; Borowicz, P.; Waluk, J.; Glasbeek, M. *J. Phys. Chem. A* **2000**, *104*, 7167.
(24) Thummel, R. P.; Hedge, V. *J. Org. Chem.* **1989**, *54*, 1720.
(25) Wu, F.; Hardesty, J.; Thummel, R. P. *J. Org. Chem.* **1998**, *63*, 4055.
(26) Wu, F.; Thummel, R. P. *Inorg. Chem.* **2000**, *39*, 584.
(27) Azawe, S. A.; Sarkis, G. Y. *J. Chem. Eng. Data* **1973**, *18*, 109.
(28) Savoia, D.; Concialini, V.; Roffia, S.; Tarsi, L. *J. Org. Chem*. **1991**, *56*, 1822.
(29) Song, E.; Wu, F.; Thummel, R. P. Manuscript in preparation.
(30) Calvin, M.; Wilmarth, W. K. *J. Am. Chem. Soc.* **1956**, *78*, 1301.
(31) Jasny, J. *J. Lumin.* **1978**, *17*, 149.
(32) Velapoldi, R. A. Considerations of Organic Compounds in Solution and Inorganic Ions in Glasses as Fluorescent Standard Reference Materials. In *National Bureau of Standards Special Publication 378, Accuracy in Spectrophotometry and Luminescence Meaurements, Proc. Conf. NBS*; NBS: Gaithersburg, MD, 1972; p 231.
(33) Frisch, M. J.; Trucks, G. W.; Schlegel, H. B.; Scuseria, G. E.; Robb, M. A.; Cheeseman, J. R.; Zakrzewski, V. G.; Montgomery, J. A., Jr.; Stratman, R. E.; Burant, J. C.; Dapprich, S.; Millam, J. M.; Daniels, A. D.; Kudin, K. N.; Strain, M. C.; Farkas, O.; Tomasi, J.; Barone, V.; Cossi, M.; Cammi, R.; Mennucci, B.; Pomelli, C.; Adamo, C.; Clifford, S.; Ochterski, J.; Petersson, G. A.; Ayala, P. Y.; Cui, Q.; Morokuma, K.; Malick, D. K.; Rabuck, A. D.; Raghavachari, K.; Foresman, J. B.; Cioslowski, J.; Ortiz, J. V.; Stefanov, B. B.; Liu, G.; Liashenko, A.; Piskorz, P.; Komaromi, I.; Gomperts, R.; Martin, R. L.; Fox, D. J.; Keith, T.; Al-Laham, M. A.; Peng, C. Y.; Nanayakkara, A.; Gonzalez, C.; Challacombe, M.; Gill, P. M. W.; Johnson, B.; Chen, W.; Wong, M. W.; Andres, J. L.; Gonzales, C.; Head-Gordon, M.; Replogle, E. S.; Pople, J. A. *Gaussian 98*, revision A.6; Gaussian, Inc.: Pittsburgh, PA, 1998.
(34) Ridley, J. E.; Zerner, M. Z. *Theor. Chim. Acta* **1973**, *32*, 111.
(35) Dewar, M. J. S.; Zoebisch, E. G.; Healy, E. F.; Stewart, J. J. P. *J. Am. Chem. Soc.* **1985**, *107*, 3902. Dewar, M. J. S.; Dieter, K. M. *J. Am. Chem. Soc.* **1986**, *108*, 8075. Stewart, J. J. P. *J. Comput.-Aided Mol. Des.* **1990**, *4*, 1.
(36) Stewart, J. J. P. *J. Comput. Chem.* **1989**, *10*, 209, 221.
(37) *Handbook of Chemistry and Physics*, 70th ed.; Weast, R. C., Lide, D. R., Astle, M. J., Beyer, W. H., Eds.; CRC Press Inc.: Boca Raton, FL, 1989−1990; p D-161.
(38) Meites, L.; Zuman, P. *Electrochemical Data*; Wiley: New York, 1974. Drushel, H. V.; Sommers, A. L. *Anal. Chem.* **1966**, *38*, 10.
(39) Headridge, D. *Electrochemical Technology for Inorganic Chemistry*; Academic Press: London, 1969.
(40) (a) Lumry, R.; Hershberger, M. *Photochem. Photobiol*. **1978**, *27*, 819. (b) Hershberger, M.; Lumry, R.; Verrall, R. *Photochem. Photobiol.* **1981**, *33*, 609. (c) Walker, M. S.; Bednar, T. W.; Lumry, R. *J. Chem. Phys.* **1967**, *47*, 1020. (d) Tamaki, T. *J. Phys. Chem.* **1983**, *87*, 2383.
(41) Gorski, A.; Waluk, J. Manuscript in preparation.
(42) Dobkowski, J.; Herbich, J.; Galievsky, V.; Thummel, R. P., Wu, F.; Waluk, J. *Ber. Bunsen-Ges. Phys. Chem.* **1998**, *102*, 469.